# Dynamics-Aware Latent Space Reachability for Exploration in Temporally-Extended Tasks

# Homanga Bharadhwaj, Animesh Garg, and Florian Shkurti

Department of Computer Science, University of Toronto
University of Toronto Robotics Institute
Vector Institute, Toronto

Abstract—Self-supervised goal proposal and reaching is a key component of efficient policy learning algorithms. Such a selfsupervised approach without access to any oracle goal sampling distribution requires deep exploration and commitment so that long horizon plans can be efficiently discovered. In this paper, we propose an exploration framework, which learns a dynamicsaware manifold of reachable states. Given a new goal, our proposed method visits a state at the current frontier of reachable states (commitment/reaching) and then explores to reach the goal (exploration). This allocates exploration budget near the frontier of the reachable region instead of its interior. We target the challenging problem of policy learning from initial and goal states specified as images, and do not assume any access to the underlying ground-truth states of the robot and the environment. To keep track of reachable latent states, we propose a distance conditioned reachability network that is trained to infer whether one state is reachable from another within the specified latent space distance. So, given an initial state, we obtain a frontier of reachable states from that state. By incorporating a curriculum for sampling easier goals (closer to the start state) before more difficult goals, we demonstrate that the proposed self-supervised exploration algorithm, can achieve 30\% superior performance on average compared to existing baselines on a set of challenging robotic environments, including on a real robot manipulation task.

## I. INTRODUCTION

Efficient exploration is one of the central open challenges in Reinforcement Learning (RL), and a key requirement for learning optimal policies, particularly in sparse-reward and long-horizon settings, where the optimization problem is difficult to solve, but easy to specify. We show that discovering policies for these settings benefits significantly from autonomous goal-setting and exploration, which requires keeping track of what regions of the state-space have been sufficiently explored and can be reached via planning, and what regions remain unknown. In this paper we present an exploration method that keeps track of reachable regions of state space and naturally handles the exploration-exploitation dilemma in sequential decision-making for unknown environments [1, 2], while being practical in real robotics settings.

For learning to plan in *unknown* environments, appropriately trading off exploration i.e. learning about the environment, and exploitation i.e. executing promising actions is the key to successful policy learning. The necessity for this trade-off is more pertinent when we want to train agents to learn autonomously in a self-supervised manner such that it is able to solve goals sampled from an unknown distribution during

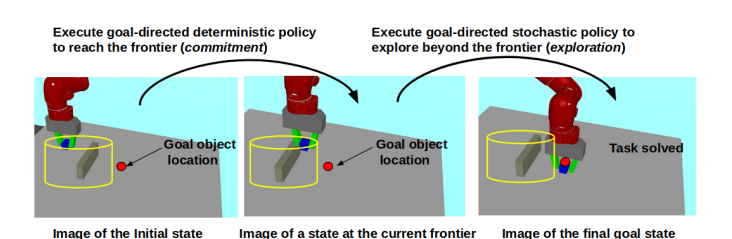
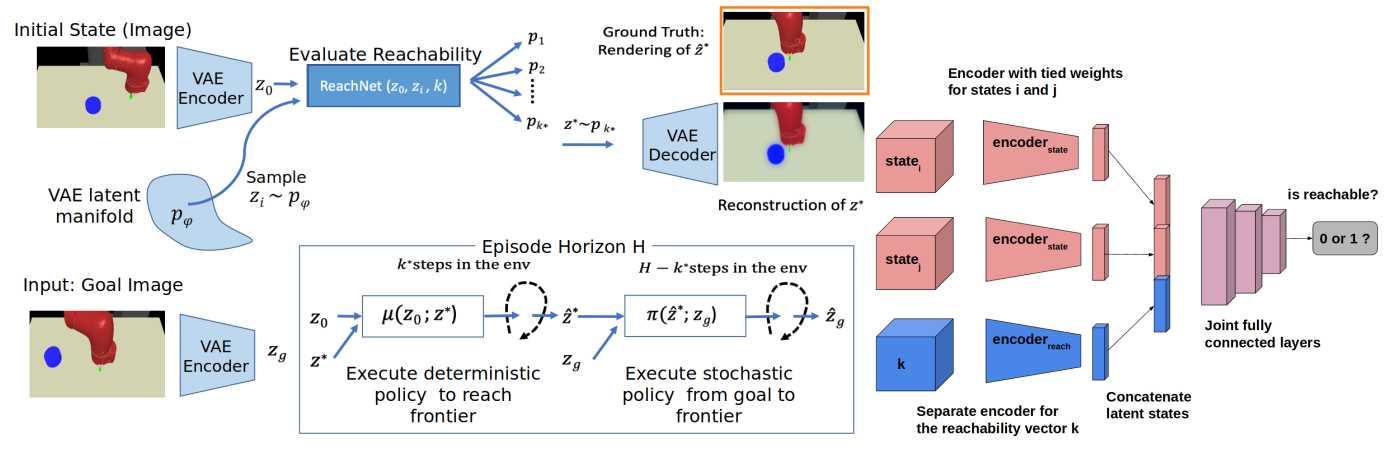


Fig. 1: Our method encourages reaching the current frontier of reachable states with a deterministic policy, and performing goal-directed exploration beyond it with a stochastic policy. In this illustration, the yellow volume corresponds to end-effector positions for the currently reachable frontier corresponding to the shown initial state.

evaluation. In this setting, during training, the agent must practice reaching self-specified random goals [3]. However, trying to specify goals through exact states of objects in the environment will require a combinatorially large representation, for explicitly randomizing different variables of the states [3, 4]. On the contrary, raw sensory signals, such as images can be used to specify goals, as has been done in recent goal-conditioned policy learning algorithms [3, 5, 6]. This paper tackles the question of how should an autonomous agent balance exploration and exploitation for goal-directed robotic tasks while learning directly from images, with no access to the ground-truth parameters of the environment during training.

The main idea of our approach is to maintain and gradually expand the frontier of reachable states by trying to reach the current frontier directly without exploring i.e. by executing a deterministic goal-conditioned policy, and exploring from beyond the current frontier in order to reach the goal by executing a stochastic goal-conditioned policy (Fig. 1). In order to achieve this, we encourage the agent to sample goals closer to the start state(s) before sampling goals that are farther away, by appropriately querying the reachability network. Planning directly in the pixel-space is not meaningful. For example, computing rewards as the pixel-wise distance between two images does not necessarily correspond to a semantically meaningful correlation with respect to how close the two ground-truth states actually are [3, 5]. Hence, we learn a latent abstraction from images, and plan in the latent space. We train a reachability network that learns whether a latent state is currently reachable from another latent state in k time-steps (k varies from 1 to the maximum length of the horizon), and use this network to compute the current frontier of reachable



(a) Forward pass of the proposed approach

(b) Reachability Network

Fig. 2: (a) An overview of our method on the Sawyer Push and Reach task. The initial and goal images are encoded by the encoder of the VAE into latents  $z_0$  and  $z_g$  respectively. Random states are sampled from the currently learned manifold of the VAE latent states, and are used to infer the current frontier  $p_{k^*}$  as described in Section IV-A. The currently learned deterministic policy is used to reach a state in the frontier  $z^*$  from the initial latent state  $z_0$ . After that, the currently learned stochastic policy is used to reach the latent goal state  $z_g$ . A reconstruction of what the latent state in the frontier  $z^*$  decodes to is shown. For clarity, a rendered view of the actual state  $z^*$  reached by the agent is shown alongside the reconstruction. (b) A schematic of the reachability network used to determine whether the latent state  $z_i$  ( $state_i$ ) is reachable from the latent state  $z_j$  ( $state_j$ ) in k time-steps. The reachability vector k consists of a vector of the same size as  $z_i$  and  $z_j$  with all its elements being k. The output 0 indicates that state  $z_i$  is not reachable from state  $z_j$ .

states given a random initial start state during training. While training the goal-conditioned policy to reach a goal latent state (corresponding to a goal image), we first execute the deterministic policy trained so far to reach a latent state at the frontier (*commitment*), and then execute the stochastic policy from beyond the frontier to reach the goal (*exploration*). We refer to this procedure of commitment to reach the frontier and exploring beyond it as *committed exploration* required for solving temporally abstracted tasks.

In summary, this paper makes the following contributions:

- We propose a dynamics-aware latent space reachability network.
- 2) We devise a policy learning scheme using the reachability network that combines deterministic and stochastic policies for committed exploration.
- 3) We empirically evaluate the proposed approach in a range of both image-based, and state-based simulation environments, and in a real robot environment. We demonstrate an improvement of 20% on average compared to state-of-the-art exploration baselines.

## II. RELATED WORKS

Vision-based RL for Robotics. Recent works have investigated vision-based learning of RL policies for specific robotic tasks like grasping [7, 8], pushing [9, 10], and navigation [11, 12], however relatively few prior works have considered the problem of learning policies in a completely self-supervised manner [3, 6]. A recent paper [4] considers RL directly from images, for general tasks without engineering a reward function, but involves a human in the loop. Some other prior works learn latent representations for RL in an unsupervised manner which can used as input to the policy, but they either require expert demonstration data [5, 13], or assume access to ground-truth states and reward functions during training [14–16]. RIG [3] proposes a general approach of first learning a

latent abstraction from images, and then planning in the latent space, but requires data collected from a randomly initialized policy to design parametric goal distributions. In addition, niether approaches do not guarantee any notion of exploration or coverage that is required for solving difficult temporally-extended tasks from minimal supervision - in particular with goals specified as raw images.

Goal-conditioned Policy Learning. While traditional model-free RL algorithms are trained to succeed in single tasks [17–20], goal-conditioned policy learning holds the promise of learning general-purpose policies that can be used for different tasks specified as different goals [3, 21–23]. However, most goal-conditioned policy learning algorithms make the stronger assumption of having access to an oracle goal sampling distribution during training [21, 22, 24, 25]. A recent paper [23] proposes an algorithm to create dynamics-aware embeddings of states, for goal-conditioned RL, but it is not scalable to images as goals (instead of ground-truth states).

Some other prior works do not assume access to an oracle goal-sampling distribution, but sample goals based on some ad-hoc heuristics like learning progress [26, 27], how off-policy the goal is [28] or sample goals randomly from the learn latent distribution over image observations [3]. Skew-Fit [6] adds structure to the goal-sampling process by sampling goals in the latent space such that the entropy over the learned distribution over states is maximized, but provides no guarantee of coverage/exploration in finite time.

**Exploration for RL.** Skew-fit [6] proposes a novel entropy maximizing objective that ensures gradual coverage in the infinite time limit. In addition, it does not incorporate any notion of commitment during exploration, which is needed to discover complex skills for solving temporally extended tasks in finite time. Go-Explore [2] addresses this issue to some extent by keeping track of previously visited states in the replay buffer, and at the start of each episode, re-setting

the environment to a previously visited state chosen on the basis of domain-specific heuristics, and continuing exploration from there. However, this approach is fundamentally limited because it assumes the environment is re-settable, which is not always feasible on a real robot. In addition, the domain-specific heuristics for Montezuma's revenge in the original paper do not readily apply to latent spaces for robotic tasks.

On the contrary, novelty/surprise based criteria have been used in many RL applications like games, and mazes [29–31]. In [29], a curiosity based intrinsic reward signal is used in addition to the external reward in order to encourage the RL agent to visit previously unvisited states. In [30], the authors explicitly keep track of the state visitation frequencies and reward the agent for visiting states with less visitation frequency. VIME [32] considers information gathering behaviors to reduce epistemic uncertainty on the dynamics model.

**Reachability and Curriculum Learning.** Our method is related to curriculum learning approaches in reinforcement learning [33–38] whereby learning easier tasks is prioritized over hard tasks, as long as measures are taken to avoid forgetting behaviors on old tasks.

**Frontier-based Exploration for Robot Mapping.** Finally, our method is intuitively similar to a large body of classic work on robot mapping, particularly frontier-based exploration approaches [39–41].

# III. PROBLEM SETUP AND BACKGROUND

# A. Problem Setup

In standard model-free RL, the objective is to learn a policy  $\pi(\cdot)$  as a function of the current state of the world  $s_t$  (this could be a latent abstraction state as well) that outputs an action  $a_t = \pi(s_t)$  to be executed in the environment, such that the expected sum of discounted returns from the environment  $R_t = \mathbb{E}_{\pi(a|s),p(s'|s,a)}[\sum_{i=t}^T \gamma^{(i-t)} r(s_i,a_i,s_{i+1})]$  is maximized. Here,  $a \in \mathcal{A}, s \in \mathcal{S}, \gamma$ , and  $r(\cdot)$  respectively denote an action in the set of actions, a state in the set of states, the discount factor, and the reward function.

**Goal-conditioned policies** This formulation is insufficient when we want to optimize expected returns with respect to different goals that can be specified at test-time. Hence, explicitly conditioning the policy on the goal  $s_g$  that must be achieved in the current episode,  $a_t = \pi(s_t; s_g)$ , and optimizing the expected sum of discounted rewards over different goals  $s_g$  sampled from the set of goals  $s_g \sim \mathcal{G}$ ,  $R_t = \mathbb{E}_{\pi(a|s;s_g),p(s'|s,a)}[\sum_{i=t}^T \gamma^{(i-t)} r(s_i,a_i,s_{i+1};s_g)]$  is a common method of learning policies that can be adapted to different goals at test time [22].

**Self-supervised learning to solve goals** We consider the setting of learning directly from images, such that the the goals are specified as images to the policy. Also, the setting is self-supervised in the sense that during training, we do not have access to any oracle goal-sampling distribution from which goals will be sampled at test-time. Hence, the agent must learn to autonomously set goals and solve them during training, in order to learn necessary re-usable skills for solving new goals sampled from an unknown distribution at test-time.

This is the setting considered in a number of recent approaches for policy learning [3, 6], and is challenging because it assumes very less information about the ground-truth environment and goal-specifications. One of the desiderata as pointed out in Skew-Fit [6] is to sample sufficiently diverse goals and learn to solve them, i.e. optimize  $\mathcal{H}(\mathcal{G}) - \mathcal{H}(\mathcal{G}|\mathcal{S})$ , where  $\mathcal{H}(\cdot)$  denotes entropy. Although this guarantees uniform coverage in the infinite limit (assuming a perfectly learned goal-reaching policy), it does not ensure deep exploration in the finite horizon case. In this paper, we emphasize the need to keep track of reachable states so to enable deep exploration via commitment, and set goals in a curriculum fashion, so that the agent learns to solve easier goals before trying to solve more difficult goals.

## B. Notation

We denote the set of observations (images) as S and the set of goals (images) as  $\mathcal{G}$ . In this paper we assume the underlying sets for S and G to be the same (any valid image can be a goal image [3, 6]) but maintain separate notations for clarity.  $f_{\psi}(\cdot)$  denotes the encoder of the  $\beta - VAE$  [42] that encodes observations  $s \sim S$  to latent states  $z \sim f_{\psi}(s)$ . The goal conditioned policy given the current latent state  $z_t$ , and the goal  $z_g$  is denoted by  $\pi_{\theta}(\cdot|z_t,z_q)$ , and  $a_t \sim \pi_{\theta}(\cdot|z_t,z_q)$  denotes the action sampled from the policy at time t. The policy  $\pi_{\theta}(\cdot|z_t,z_q)$ consists of a deterministic component  $\mu_{\theta}(\cdot|z_t,z_q)$ , and a noise term  $\epsilon$ , such that  $\pi_{\theta}(\cdot|z_t,z_g) = \mu_{\theta}(\cdot|z_t,z_g) + \sigma_{\theta}\epsilon$ , where  $\epsilon$  is a Gaussian  $\mathcal{N}(0,\mathbf{I})$  in this paper.  $ReachNet(z_i,z_i;k)$ denotes the reachability network that takes as input two latent states  $z_i$ , and  $z_j$  and is conditioned on a reachability integer  $k \in [1,..,H]$ , where H is the maximum time horizon of the episode. The output of  $ReachNet(z_i, z_i; k)$  is either a 0 denoting  $z_i$  is currently not reachable from  $z_i$  (and vice-versa) or a 1 denoting  $z_i$  is reachable from  $z_i$  (and vice-versa).

We consider the problem setting where a robot is initialized to a particular configuration, and is tasked to reach a goal, specified as an image. The test time goal distribution, from which goal images will be sampled for evaluation is not available during training, and hence the training approach is completely self-supervised. The underlying distribution of observations  $\mathcal S$  is same as the underlying distribution of goals  $\mathcal G$  during training, and are distributions over images from a camera.

## IV. OUR APPROACH

In this section, we discuss the specifics of the proposed approach, summarized in Algorithm 1.

## A. Our Method's Key Insight

Consider the goal conditioned policy  $\pi(\cdot|z_t,z_g)$  with an initial latent state  $z_0$ , and a goal latent state  $z_g$ . The key idea of our method is to do committed exploration, by directly going to the frontier of reachable states for  $z_0$  by executing the deterministic policy  $\mu_{\theta}(\cdot|z_t,z_{k^*})$  and then execute the exploration policy  $\pi_{\theta}(\cdot|z_t,z_g)$  from the frontier to perform goal directed exploration for the actual goal  $z_g$ . The frontier defined by  $p_{k^*}$  is the empirical distribution of states that can

be reliably reached from the initial state, and are the farthest away from the initial state, in terms of the minimum number of timesteps needed to visit them. The timestep index  $k^*$  that defines how far away the current frontier is, can be computed as follows:

$$k^* = \underset{k}{\operatorname{arg\,max}}(IsReachable(z_0; k))$$

The binary predicate  $IsReachable(z_0; k)$  keeps track of whether the fraction of states in the empirical distribution of k-reachable states  $p_k$  is above a threshold  $1 - \delta$ . The value of  $IsReachable(z_0;k) \ \forall k \in [1,..,H]$  before the start of the episode from  $z_0$  is computed as:

$$= \begin{cases} True, & \text{if } \mathbb{E}_{z \sim p_{\phi}(z)} ReachNet(z_0, z; k) \ge 1 - \delta \\ False, & \text{otherwise} \end{cases}$$
 (1)

Here  $p_{\phi}(z)$  is the current probability distribution of latent states as learned by the  $\beta - VAE$  [42] with encoder  $f_{ab}(\cdot)$ .  $\delta$  is set to 0.2. For computing  $\mathbb{E}_{z \sim p_{\phi}(z)} ReachNet(z_0, z; k)$ above, we randomly sample states  $z \sim p_{\phi}(z)$  from the latent manifold of the VAE, the intuition of which is illustrated in Fig. 3. After calculating all the predicates  $IsReachable(z_0; k)$  $\forall k \in [1,...,H]$  and determining the value of  $k^*$ , we sample a state  $z_{k^*}$  from the empirical distribution of  $k^*$ -reachable states,  $p_{k^*}$ , ensuring that it does not belong to any  $p_k \ \forall k < k^*$ . Here, the empirical distribution  $p_k$  denotes the set of states zin the computation of  $\mathbb{E}_{z \sim p_{\phi}(z)} ReachNet(z_0, z; k)$  for which  $ReachNet(z_0, z; k)$  returns a 1, and  $ReachNet(z_0, z; k')$ returns a 0,  $\forall k' < k$ .

In order to ensure that the sampled state  $z_{k^*}$  is the closest possible state to the goal  $z_q$  among all states in the frontier  $p_{k^*}$ , we perform the following additional optimization

$$z_{k^*} = \arg\min_{z > r_{k,k}} ||z - z_g||_2 \tag{2}$$

 $z_{k^*} = \mathop{\arg\min}_{z \sim p_{k^*}} ||z-z_g||_2 \tag{2}$  Here,  $||\cdot||_2$  denotes the  $L_2$  norm. The above optimization encourages choosing the state in the frontier that is closest to the latent goal state  $z_q$ .

Our method encourages committed exploration because the set of states until the frontier  $p_{k^*}$  have already been sufficiently explored, and hence the major thrust of exploration should be beyond that, so that new states are rapidly discovered. The SkewFit [6] approach showed that if the distribution over states is skewed to highly weigh rare states, and goals are sampled from this skewed distribution, the entropy over states  $\mathcal{H}(\mathcal{S})$  will eventually approach the entropy of a uniform distribution  $U_S$  over the states. However, this is guaranteed in the infinite time limit. Applying our method with the SkewFit trick for sampling goals will still maintain the guarantee of maximum entropy, but improve sample efficiency of policy learning. Algorithm 1 shows an overview algorithm for our method. In our specific implementation, we use SAC [18] as the base off-policy model-free RL algorithm for minimizing the Bellman Error in the overall algorithm that is described in the Appendix.

## B. Training the Reachability Network

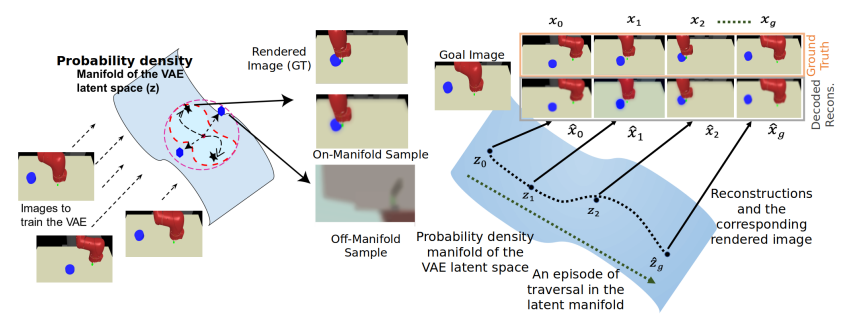
The reachability network  $ReachNet(z_i, z_i; k)$  is a feedforward neural network with fully connected layers and ReLU Algorithm 1 Overview of the proposed Algorithm (Subroutines and the complete Algorithm are in the Appendix)

```
1: procedure OVERALL(GCP \mu_{\theta}, \pi_{\theta}, Prior p(z), S, f_{\psi}(\cdot),
    IsReachable(\cdot), H_0, N, \epsilon, \delta, ReplayBuffer \mathcal{B})
 2:
         p_{\phi} = p(z)
 3:
         Init ReachNet(\cdot,\cdot;k), Def ReachData \mathcal{D}, K = H_0N
         for episodes = 1 to N do
 4:
              s_0 \sim S_0, encode z_0 = f_{\psi}(s_0), z_q \sim p_{\phi}, \hat{z}^* = z_0
 5:
              if episodes \geq N/4 then
 6:
                  for k = K - 1, ..., 1 do
 7:
                       Set the value of IsReachable(z_0; k)
 8:
                  k^* = \arg\max_{k} (IsReachable(z_0; k))
 9:
10:
                  Choose z_{k^*} = \operatorname{arg\,min}_{z \sim p_{k^*}} ||z - z_g||_2
                  Exec \pi_{\theta}(z_0; z_{k^*}), reach \hat{z}^* s.t. ||\hat{z}^* - z_{k^*}|| \approx 0
11:
12:
              Set H = H_0 * episodes // Curriculum
13:
              for t = 0, ..., H - 1 do
                  if t == 0 then
14:
                       Select a_t \sim \mu_{\theta}(\hat{z}^*; z_q) and execute it
15:
                  if t > 0 and t < k^* then
16:
                       Select a_t \sim \mu_{\theta}(f_{\psi}(s_t); z_g) and execute it
17:
                  if t > 0 and t > k^* then
18:
                       Select a_t \sim \pi_{\theta}(f_{\psi}(s_t); z_g) and execute it
19:
                  // Store tuple and Train policy
20:
21:
                  STOREANDTRAIN()
              APPENDTODATASET(\mathcal{D})
22:
              SAMPLEFUTURESTATES(\mathcal{B})
23:
              Construct skewed dist. p_{skewed} from \mathcal{B} (Skew-Fit)
24:
25:
              Train the encoder using p_{\phi} = p_{skewed}
              Train ReachNet(\cdot,\cdot;k) using ReachDataset \mathcal{D}
26:
```

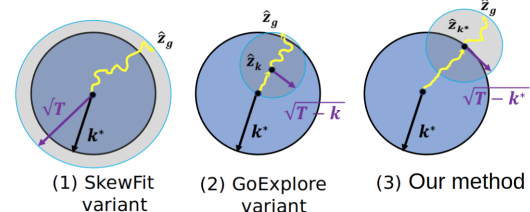
non-linearities, the architecture of which is shown in Fig. 2, with details in the Appendix. The architecture has three basic components, two encoders ( $encoder_{state}$ ,  $encoder_{reach}$ ), one decoder, and one concatenation layer. The latent states  $z_i, z_j$ are encoded by the same encoder encoder state (i.e. two encoders with tied weights, as in a Siamese Network [43]) and the reachability value k is encoded by another encoder  $encoder_{reach}$ . In order to ensure effective conditioning of the network ReachNet on the variable k, we input a vector of the same dimension as  $z_i$  and  $z_j$ , with all of its values being  $k, \mathbf{k} = [k, k, ..., k].$ 

It is important to note that such neural networks conditioned on certain vectors have been previously explored in literature, e.g. for dynamics conditioned policies [44]. The three encoder outputs, corresponding to  $z_i, z_j$ , and k are concatenated and fed into a series of shared fully connected layers, which we denote as the decoder. The output of  $ReachNet(z_i, z_i; k)$  is a 1 or a 0 corresponding to whether  $z_i$  is reachable from  $z_i$ in k steps or not, respectively.

To obtain training data for ReachNet, while executing rollouts in each episode, starting from the start state  $z_0$ , we keep track of the number of time-steps needed to visit every latent state  $z_i$  during the episode. We store tuples of the



(a) (1) Our method samples latent goals from the the probability density manifold of the learned VAE latent space  $p_{\phi}(z)$ . Sampling states from outside the manifold (i.e. sampling z with low probability density under  $p_{\phi}(z)$ ) is likely to correspond to images (upon decoding) that do not correspond to a dynamically feasible image of a simulator state. For example, in this figure, given some latent state in the manifold (shown by the center of the sphere), states outside the manifold correspond to regions of the sphere (outlined in pink) that do not intersect the manifold (the intersection is outlined in red). (2) The second figure shows how sampling goals that lie on the latent VAE manifold and traversing on the latent manifold leads to latent states that decode to realistic dynamically feasible image frames.



(b) The blue area of radius  $k^*$  denotes the already sufficiently explored region such that  $k^*$  is the current frontier. T is the max. number of timesteps of the episode. (3) shows the case when the deterministic goal reaching policy takes the agent to a state at the frontier in  $k^*$  steps, and after that it executes the stochastic policy for  $T-k^*$  steps. (2) shows the case when the agent first goes to a random previously visited state, by executing a deterministic goal reaching policy (say, for k steps), and then executes the stochastic policy for T-k steps. (1) shows the case when the agent executes the stochastic policy for T steps starting at the origin. The simplified Go-Explore [2] and SkewFit [6] models are described in Section V

Fig. 3: (a) Sampling from the VAE probability density manifold and traversal in the VAE latent space. (b) Simplified analysis of Our method.

form  $(z_i, z_j, k_{ij}) \ \forall i < j$  in memory, where  $k_{ij} = j - i$ , corresponding to the entire episode. Now, to obtain labels  $\{0,1\}$  corresponding to the input tuple  $(z_i, z_j, k)$ , we use the following heuristic:

$$label(z_i, z_j, k) = \begin{cases} 1, & \text{if } |k_{ij} > \alpha k| \\ 0, & \text{if } |k_{ij} < k| \end{cases}$$
 (3)

Here  $\alpha \in [1.2, 1.5)$  is a threshold to ensure sufficient separation between positive and negative examples.

## C. Implicit Curriculum for Increasing the Frontier

The idea of growing the set of reachable states during training is vital to ReaxhExplore. Hence, we leverage curriculum to ensure that in-distribution nearby goals are sampled before goals further away. This naturally relates to the idea of a curriculum [45], and can be ensured by gradually increasing the maximum horizon H of the episodes. So, we start with a horizon length of  $H=H_0$  and gradually increase it to  $H=NH_0$  during training, where N is the total number of episodes.

In addition to this, while sampling goals we also ensure that the chosen goal before the start of every episode does not lie in any of the  $p_k$  distributions, where  $k \leq k^*$  corresponding to the calculated  $k^*$ . This implies that the chosen goal is beyond the current frontier, and hence would require exploration beyond what has been already visited.

# V. ANALYSIS OF REACHEXPLORE: INTUITION OF DEEP EXPLORATION THROUGH AVERAGE CASE ANALYSIS

In this section, we provide formal analysis of ReachExplore in a simplified, idealized, setting. Consider a 2D world with a single start location  $\mathbf{z}_0$  and and let the goal be denoted by  $\mathbf{z}_g$ . Let  $p_{k^*}$  denote the current frontier. Let T denote the total time-steps in the current episode.

We aim to show that using this time-step budget, the odds of exploring previously unvisited states farther away from the start state are higher when using ReachExplore, as compared to without using it. For simplicity, we assume the stochastic goal-reaching policy to be the policy of a random walker, and the deterministic goal-reaching policy to be near-optimal in the sense that given a target goal in  $p_{k^*}$ , and an initial state in the already explored region, it can precisely reach the target location at the frontier with a high probability( $\gg 0$ ).

For analysis, we define SkewFit [6], GoExplore [2], and our method in the above setting to be the following simplified schemes, and illustrate the same in Fig. 3b:

- 1) **SkewFit-variant:** The model that executes the stochastic policy for the entire length T of the episode to reach goal  $z_g$ , and sets diverse goals at the start of every episode, as per the SkewFit objective [6].
- 2) **GoExplore-variant:** The model that first chooses a random previously visited intermediate latent goal state from the archive (not necessarily from the frontier  $p_{k^*}$ ), executes a deterministic goal directed policy for say k steps to reach the intermediate goal, and then executes the stochastic policy exploring for the next T k steps. For analysis,  $0 < k < k^*$ . This is similar in principle to the idea of Go-Explore [2]<sup>1</sup>. It also sets diverse goals at the start of every episode, as per the SkewFit objective [6].
- 3) Our method: The model that first chooses a state from the frontier  $p_{k^*}$ , executes a deterministic goal directed policy for say  $k^*$  steps to reach the frontier, and then

 $^1$ Here, we refer to the intuition of Phase 1 of Go-Explore, where the idea is to "select a state from the archive, go to that state, start exploring from that state, and update the archive." For illustration and analysis, we do not consider the exact approach of Go-Explore. In order to "go to that state" Go-Explore directly resets the environment to that state, which is not allowed in our problem setting. Hence, in Fig. 3b, we perform the analysis with a goal-directed policy to reach the state. Also, since Go-Explore does not keep track of reachability, we cannot know whether the intermediate goal chosen can be reached in k timesteps. But for analysis, we assume the intermediate goal is chosen from some  $p_k$  distribution as described in Section IV-A

executes the stochastic policy exploring for the next  $T-k^*$  steps. It also sets diverse goals at the start of every episode, as per the SkewFit objective [6].

**Lemma V.1.** For a random walk with unit step size in 2D (in a plane), the average distance away from a point (say, the origin) traversed in t time-steps is  $\sqrt{t}$ .

*Proof.* The proof of is provided in the Appendix.

QED

The subsequent results are all based on the above stated lemma and assumptions.

**Lemma V.2.** Starting at  $z_0$  and assuming the stochastic goal-reaching policy to be a random walk, on average the SkewFit scheme will reach as far as  $R_1 = \sqrt{T}$  at the most in one episode.

*Proof.* This follows directly from Lemma V.1 by setting t = T, where T is the max. number of timesteps in the episode.

QED

**Lemma V.3.** Starting at  $z_0$  and assuming the deterministic goal-deterministic policy to be near optimal (succeeds with a very high probability>> 0), and the stochastic goal-reaching policy to be a random walk, on average GoExplore scheme will be bounded by  $R_2 = \frac{1}{k^*} (\sum_{k=0}^{k^*} (k + \sqrt{T-k}))$  in one episode.

*Proof.* Since GoExplore first goes to a random previously visited state using the deterministic goal conditioned policy, from Fig 3b it is evident that the distance of such a state from the start state could be in the range  $(0, k^*)$ . Let this distance be k. Then, from Lemma V.1, the max distance on average traversed by the agent from  $z_0$ , if the intermediate state is at a distance k, can be given as:

$$r_k = k + \sqrt{T - k}$$

Averaging over all the distance of all possible intermediate positions  $k \in (0, k^*)$ , we obtain the final averaged maximum distance reached by the agent in one episode as:

$$R_2 = \frac{1}{k^*} \sum_{k=0}^{k^*} (k + \sqrt{T - k})$$
 QED

**Lemma V.4.** Starting at  $z_0$  and assuming the deterministic goal-conditioned policy to be near optimal (succeeds with a very high probability >> 0), and the stochastic goal-reaching policy to be a random walk, on average our method will be bounded by  $R_3 = k^* + \sqrt{T - k^*}$ 

*Proof.* In the proof for lemma V.3, setting  $k=k^*$  in the formula, for  $r_k$  gives us the maximum average distance for our method as:

$$R_3 = k^* + \sqrt{T - k^*}$$

QED

**Theorem V.5.**  $R_3 > R_2 \ \forall k^* \in [1,T)$  and  $R_3 > R_1 \ \forall k^* \in [1,T)$ . i.e. After the frontier  $k^*$  is sufficiently large,

the maximum distance from the origin reached by our method is more than both GoExplore and SkewFit.

*Proof.* We provide the proof of this in the Appendix. QED

Theorem V.5 is the main result of our analysis and it intuitively suggests the effectiveness of deep exploration guaranteed by our method. This is shown through a visualization in Fig. 3b.

In Fig. 3b (2) and (3), we assume the deterministic policy succeeds with high probability( $\gg$  0), which is usually the case after sufficient training iterations in off-policy Q-learning. It can be easily seen that if  $k^*$  increases during training (i.e. the reachable frontier expands), then after a finite number of interactions with the environment, we will have  $k^* > \sqrt{T}$ . We ensure that this happens because of the implicit curriculum on horizon length, and the sampling of goals beyond the current reachable frontier at the start of every episode.

## VI. EXPERIMENTS

Our experiments aim to understand the following questions: (1) How does our method compare to existing state-of-theart exploration baselines, in terms of faster convergence and higher cumulative success? (2) How does our method scale as task complexity increases? (3) Can our method scale to tasks on a real robotic arm?

#### A. Environments

We consider the image-based and state-based environments illustrated in Fig. 4. In case of image-based environments, the initial state and the goal are both specified as images. In case of state-based environments, the initial state and the goal consists of the coordinates of the object(s), the position and velocity of different components of the robotic arm, and other details as appropriate for the environment (Refer to the Appendix for details). In both these cases, during training, the agent does not have access to any oracle goal-sampling distribution. In Fig. 4, (b), and (c) are configured to be sparsereward settings, where the reward is 1 only when the agent solves the goal and is 0 otherwise. To define when a goal is solved, for each environment there is a certain threshold distance between the agent's final state and the goal state, the details of which are mentioned in the appendix. All the other environments in Fig. 4 use only a latent distance based reward during training (reward  $r = -||z_t - z_q||_2$ ;  $z_t$  is the agent's current latent state and  $z_q$  is the goal latent state), and have no access to ground-truth simulator states.

- 1) **Pointmass Navigation** (*Image-based*): A pointmass object must be navigated from an initial location to a goal location in the presence of obstacles. The agent must plan a temporally extended path that would occassionally involve moving away from the goal. This is a 2D environment with a continuous action space, and the agent has access to images from a top-down view.
- 2) Fetch Slide (State-based): A Fetch robot arm must be controlled to push and slide a puck on the table such that it reaches a certain goal location. It is ensured that sliding must happen (and not just pushing) because the

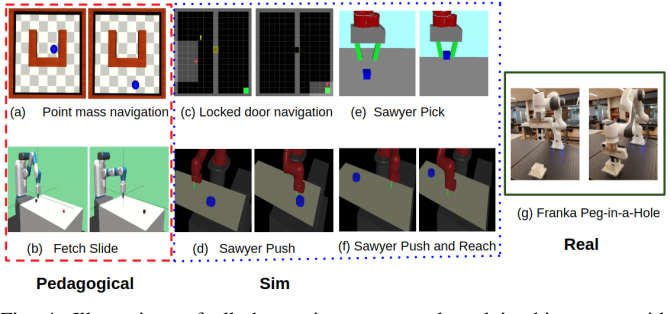


Fig. 4: Illustrations of all the environments evaluated in this paper, with example initial (left) and goal (right) images. Each environment we consider is meant to demonstrate scaling of the proposed approach to different settings: image-based goals, state-based goals, continuous action spaces, discrete action spaces, different dynamics (point mass, Fetch robot, Sawyer robot, Franka Panda robot), increasing task complexity (Push to Push and Reach), and applicability to a real robot. Details are in the Appendix.

goal location is beyond the reach of the arm's end-effector. We make this environment significantly difficult by reducing the default friction coefficient by a factor of 2. The agent has access to state information - the position (x,y,z) and velocity  $(v_x,v_y,v_z)$  of its end-effector.

- 3) **Gridworld Locked Door Navigation** (*Image-based*): A point agent navigates a maze to pick up a key, open a locked door, and navigate to a goal location on the other side of the door. This is a 2D environment, and the agent has access to a top-down view. At each timestep, the agent has the option to choose from six actions (so discrete action space).
- 4) **Sawyer Pick** (*Image-based*): A Sawyer robot arm must be controlled to pick a puck from a certain location and lift it to a target location above the table. The agent has access to images from a camera mounted on the arm.
- 5) **Sawyer Push** (*Image-based*): A Sawyer robot must push a puck to a certain location with the help of its endeffector. The agent has access to images from a camera mounted on the arm.
- 6) Sawyer Push and Reach (Image-based): A Sawyer robot arm is controlled to push a puck to a target location, and move its end-effector to a (different) target location. The agent has access to images from a camera mounted on the arm.
- 7) Franka Panda Peg in a Hole (State-based; Real robot); A real Franka Panda arm must be controlled to place a peg in a hole. The agent is velocity controlled and has access to state information the position (x, y, z) and velocity  $(v_x, v_y, v_z)$  of its end-effector.

## B. Setup

We use the Pytorch library [46, 47] in Python for implementing our algorithm, and ADAM [48] for optimization. We consider two recent state-of-the-art exploration algorithms, namely Skew-Fit [6], and Go-Explore [2] as our primary baselines for comparison. For both these baselines, for consistency, we use SAC for policy-learning. Based on the original implementation of Go-Explore [2], we create a version using

SAC [18] as the base policy and employing the Go-Explore trick which we use as our baseline.

For training, we train our method and the baselines in a completely unsupervised manner, without access to any oracle goal-sampling distribution. In addition, in the image-based environments, during training the agent does not have access to any prior information about the state-space. In order to *evaluate* the performance of the algorithms, we sample goal images from a uniform distribution over valid images and report the final distance of the agent to the corresponding states in simulator. This method of evaluation, although applicable only in simulation, is a reliable metric for RL with vision-based goals, as described in prior works [3, 6]. It is important to note that we access the simulator states only for *evaluation* - not for training (except for (b), and (h) in Fig. 4).

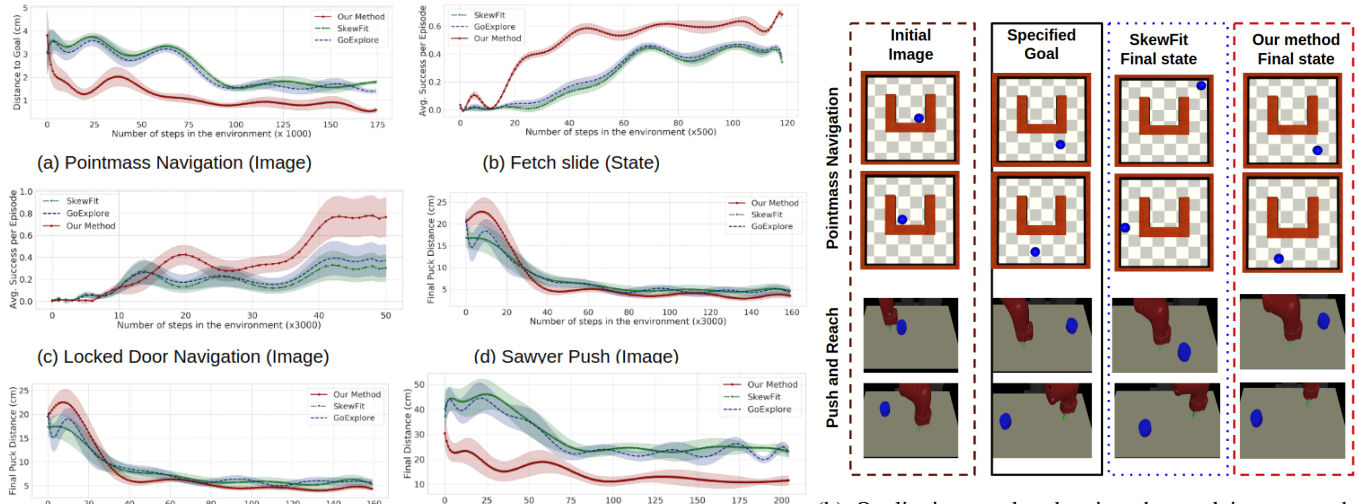
## C. Results

Our method achieves higher success during evaluation in reaching closer to the goals compared to the baselines Fig. 5 shows comparisons of our method against the baseline algorithms on all the robotic simulation environments. It is evident that our method performs significantly better than all the baselines. The image based Sawyer Push and Reach environment is challenging because there are two components to the overall task. The significant performance improvement of our method over the baselines can be can be clearly seen in Fig. 5.

The pointmass navigation environment is challenging because during evaluation, we choose the initial position to be inside the U-shaped area, and the goal location to be outside it, and the agent does not know this apriori. So, during training the agent must learn to set difficult goals outside the black arena and must try to solve them. This requires deep committed exploration, and as shown in Fig. 5a, our method succeeds in achieving this.

In addition to the image based goal environments, we consider a challenging state-based goal environment as proof-of-concept to demonstrate the effectiveness of our method. In Fig. 5a we see that for the slide task on a Fetch robot, our method achieves much higher success rate compared to the baselines in pushing the puck with the right amount of force in the right direction such that it stops exactly at the goal location. In order to succeed in this task, the agent must acquire an implicit estimate of the friction coefficient between the puck and the table top, and hence must learn to set goals close and solve them before setting goals farther away.

Our method scales to tasks of increasing complexity From Fig. 5a, we see that our method performs comparably to its baselines. The improvement of our method over SkewFit is not statistically significant. However, in the task of Push and Reach (Fig. 5a) we observe significant improvement of our method over SkewFit. The baselines succeed either in the push part of the task or the reach part of the task but not both, suggesting overly greedy policies without long term consideration (Refer qualitative results in Fig. 5b). This suggests the effectiveness of our method in scaling to a difficult task that requires more



(a) Comparative results on simulation environments

(b) Qualitative results showing the goal image on the left, and rendered images of the final states reached by SkewFit and our method for two evaluation runs in two different environments.

Fig. 5: Comparison of our method and SkewFit on an ensemble of vision-based and state-based simulation environments. In the vision based environments, the goal is specified as an image and ground truth states of the simulation are not used at all during training. The error bars are with respect to three random seeds. It is important to emphasize that the training proceeds in a completely self-supervised manner, without assuming any access to the oracle goal sampling distribution. The results reported are for evaluations on test suites (initial and goal images are sampled from a test distribution unknown to the agent) as training progresses. Although the ground-truth simulator states are not accessed during training (for (a), (c), (d), (e), and (f)), for the evaluation reported in these figures, we measure the ground truth  $L_2$  norm of the final distance of the object/end-effector (as appropriate for the environment) from the goal location. In (f), we evaluate the final distance between the (puck+end-effector)'s location and the goal location. In (c), success is measured as +1 if the agent reaches the final green goal square in the grid, and 0 otherwise. In (b), success is measured as +1 if the puck reaches within 2cm of the goal location. In (a), (d), (e), and (f). lower is better. In (b) and (c), higher is better.

(f) Sawyer Push and Reach (Image)

temporal abstraction. This benefit is probably because our method performs two staged exploration, which enables it to quickly discover regions that are farther away from the initial state given at the start of the episode.

(e) Sawyer Pick (Image)

We observe similar behaviors of scaling to more complicated tasks by looking at the results of the Pointmass Navigation in Fig. 5a. While the task can be solved even by simple strategies when the goal location is within the U-shaped ring, the agent must actually discover temporally abstracted trajectories when the goal location is outside the U-shaped ring. Discovering such successful trajectories in the face of only latent rewards, and no ground-truth reward signals further demonstrates the need for committed exploration.

Our method scales to tasks on a Real Franka Panda **robotic arm** Fig. 6 shows results for our method on a peg-ina-hole evaluated on the Franka Panda arm. Here the objective is to insert a peg into a hole, an illustration of which is shown in Fig. 4. The reward function is defined to be the negative of the distance from the center of bottom of the peg to the center of the bottom of the hole. There is an additional heavy reward penalty for 'collision' and a mild penalty for 'contact.' The home position of the panda arm (to which it is initialized) is such that the distance from the center of the bottom of the peg to the center of the bottom of the hole is 0.35 meters. The heavy penalty for collision is -10 and the mild penalty for contact is -1. We can observe from Fig. 6 that our method successfully solves the task while the baseline GoExplore does not converge to the solution. This demonstrates the applicability of our method on a real robotic

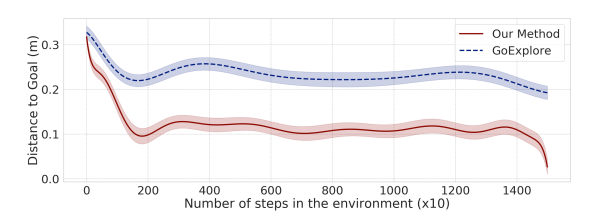


Fig. 6: Results of a Peg-in-a hole task on the real Franka Emika Panda arm. The evaluation metric on the y-axis is the distance  $(L_2 \text{ norm})$  of the center of the bottom of the hole from the center of the bottom of the peg. The state consists of the position and velocities of the end-effector. Lower is better

arm.

## VII. CONCLUSION

In this paper we proposed an algorithm for committed exploration, by keeping track of the frontier of reachable states, and during the start of every episode, executing a deterministic goal-conditioned policy to reach the current frontier, followed by executing a stochastic goal-conditioned exploration policy to reach the goal. The proposed approach can work directly over image-based observations and goal specifications, does not require any reward signal from the environment during training, and is completely self-supervised in that it does not assume access to the oracle goal-sampling distribution for evaluation. Through experiments on eight environments with varying characteristics, task complexities, and temporal abstractions, we demonstrate the efficacy of the proposed approach over state of the art exploration baselines.

#### REFERENCES

- [1] L. Zintgraf, K. Shiarlis, M. Igl, S. Schulze, Y. Gal, K. Hofmann, and S. Whiteson, "Varibad: A very good method for bayes-adaptive deep rl via meta-learning," 2019.
- [2] A. Ecoffet, J. Huizinga, J. Lehman, K. O. Stanley, and J. Clune, "Go-explore: a new approach for hard-exploration problems," *arXiv preprint arXiv:1901.10995*, 2019.
- [3] A. V. Nair, V. Pong, M. Dalal, S. Bahl, S. Lin, and S. Levine, "Visual reinforcement learning with imagined goals," in *Advances in Neural Information Processing Systems*, pp. 9191–9200, 2018.
- [4] A. Singh, L. Yang, K. Hartikainen, C. Finn, and S. Levine, "End-to-end robotic reinforcement learning without reward engineering," *arXiv* preprint *arXiv*:1904.07854, 2019.
- [5] A. Srinivas, A. Jabri, P. Abbeel, S. Levine, and C. Finn, "Universal planning networks," arXiv preprint arXiv:1804.00645, 2018.
- [6] V. H. Pong, M. Dalal, S. Lin, A. Nair, S. Bahl, and S. Levine, "Skew-fit: State-covering self-supervised reinforcement learning," arXiv preprint arXiv:1903.03698, 2019.
- [7] L. Pinto, M. Andrychowicz, P. Welinder, W. Zaremba, and P. Abbeel, "Asymmetric actor critic for image-based robot learning," arXiv preprint arXiv:1710.06542, 2017.
- [8] L. Pinto and A. Gupta, "Supersizing self-supervision: Learning to grasp from 50k tries and 700 robot hours," in 2016 IEEE international conference on robotics and automation (ICRA), pp. 3406–3413, IEEE, 2016.
- [9] C. Finn and S. Levine, "Deep visual foresight for planning robot motion," in 2017 IEEE International Conference on Robotics and Automation (ICRA), pp. 2786– 2793, IEEE, 2017.
- [10] P. Agrawal, A. V. Nair, P. Abbeel, J. Malik, and S. Levine, "Learning to poke by poking: Experiential learning of intuitive physics," in *Advances in Neural Information Processing Systems*, pp. 5074–5082, 2016.
- [11] S. Lange, M. Riedmiller, and A. Voigtländer, "Autonomous reinforcement learning on raw visual input data in a real world application," in *The 2012 International Joint Conference on Neural Networks (IJCNN)*, pp. 1–8, IEEE, 2012.
- [12] D. Pathak, P. Mahmoudieh, G. Luo, P. Agrawal, D. Chen, Y. Shentu, E. Shelhamer, J. Malik, A. A. Efros, and T. Darrell, "Zero-shot visual imitation," in *Proceedings* of the IEEE Conference on Computer Vision and Pattern Recognition Workshops, pp. 2050–2053, 2018.
- [13] H. Bharadhwaj, Z. Wang, Y. Bengio, and L. Paull, "A data-efficient framework for training and sim-toreal transfer of navigation policies," in 2019 International Conference on Robotics and Automation (ICRA), pp. 782–788, IEEE, 2019.
- [14] D. Ha and J. Schmidhuber, "World models," arXiv

- preprint arXiv:1803.10122, 2018.
- [15] C. Finn, X. Y. Tan, Y. Duan, T. Darrell, S. Levine, and P. Abbeel, "Deep spatial autoencoders for visuomotor learning," in 2016 IEEE International Conference on Robotics and Automation (ICRA), pp. 512–519, IEEE, 2016.
- [16] M. Watter, J. Springenberg, J. Boedecker, and M. Ried-miller, "Embed to control: A locally linear latent dynamics model for control from raw images," in *Advances in neural information processing systems*, pp. 2746–2754, 2015.
- [17] S. Fujimoto, H. van Hoof, and D. Meger, "Addressing function approximation error in actor-critic methods," arXiv preprint arXiv:1802.09477, 2018.
- [18] T. Haarnoja, A. Zhou, P. Abbeel, and S. Levine, "Soft actor-critic: Off-policy maximum entropy deep reinforcement learning with a stochastic actor," *arXiv preprint arXiv:1801.01290*, 2018.
- [19] J. Schulman, F. Wolski, P. Dhariwal, A. Radford, and O. Klimov, "Proximal policy optimization algorithms," arXiv preprint arXiv:1707.06347, 2017.
- [20] J. Schulman, S. Levine, P. Abbeel, M. Jordan, and P. Moritz, "Trust region policy optimization," in *Interna*tional conference on machine learning, pp. 1889–1897, 2015.
- [21] L. P. Kaelbling, "Learning to achieve goals," in *IJCAI*, pp. 1094–1099, Citeseer, 1993.
- [22] M. Andrychowicz, F. Wolski, A. Ray, J. Schneider, R. Fong, P. Welinder, B. McGrew, J. Tobin, O. P. Abbeel, and W. Zaremba, "Hindsight experience replay," in *Advances in Neural Information Processing Systems*, pp. 5048–5058, 2017.
- [23] D. Ghosh, A. Gupta, and S. Levine, "Learning actionable representations with goal-conditioned policies," arXiv preprint arXiv:1811.07819, 2018.
- [24] T. Schaul, D. Horgan, K. Gregor, and D. Silver, "Universal value function approximators," in *International Conference on Machine Learning*, pp. 1312–1320, 2015.
- [25] S. Nasiriany, V. Pong, S. Lin, and S. Levine, "Planning with goal-conditioned policies," in *Advances in Neural Information Processing Systems*, pp. 14814–14825, 2019.
- [26] C. Colas, O. Sigaud, and P.-Y. Oudeyer, "Curious: Intrinsically motivated multi-task, multi-goal reinforcement learning," *arXiv preprint arXiv:1810.06284*, 2018.
- [27] V. Veeriah, J. Oh, and S. Singh, "Many-goals reinforcement learning," *arXiv preprint arXiv:1806.09605*, 2018.
- [28] O. Nachum, S. S. Gu, H. Lee, and S. Levine, "Data-efficient hierarchical reinforcement learning," in *Advances in Neural Information Processing Systems*, pp. 3303–3313, 2018.
- [29] D. Pathak, P. Agrawal, A. A. Efros, and T. Darrell, "Curiosity-driven exploration by self-supervised prediction," in *Proceedings of the IEEE Conference on Com*puter Vision and Pattern Recognition Workshops, pp. 16– 17, 2017.
- [30] M. G. Bellemare, S. Srinivasan, G. Ostrovski,

- T. Schaul, D. Saxton, and R. Munos, "Unifying count-based exploration and intrinsic motivation," *CoRR*, vol. abs/1606.01868, 2016.
- [31] D. Korenkevych, A. R. Mahmood, G. Vasan, and J. Bergstra, "Autoregressive policies for continuous control deep reinforcement learning," arXiv preprint arXiv:1903.11524, 2019.
- [32] R. Houthooft, X. Chen, Y. Duan, J. Schulman, F. D. Turck, and P. Abbeel, "Curiosity-driven exploration in deep reinforcement learning via bayesian neural networks," *CoRR*, vol. abs/1605.09674, 2016.
- [33] V. R. Royo, D. Fridovich-Keil, S. L. Herbert, and C. J. Tomlin, "Classification-based approximate reachability with guarantees applied to safe trajectory tracking," *CoRR*, vol. abs/1803.03237, 2018.
- [34] D. Held, X. Geng, C. Florensa, and P. Abbeel, "Automatic goal generation for reinforcement learning agents," *CoRR*, vol. abs/1705.06366, 2017.
- [35] J. L. Elman, "Learning and development in neural networks: the importance of starting small," *Cognition*, vol. 48, no. 1, pp. 71 99, 1993.
- [36] OpenAI, I. Akkaya, M. Andrychowicz, M. Chociej, M. Litwin, B. McGrew, A. Petron, A. Paino, M. Plappert, G. Powell, R. Ribas, J. Schneider, N. Tezak, J. Tworek, P. Welinder, L. Weng, Q. Yuan, W. Zaremba, and L. Zhang, "Solving rubik's cube with a robot hand," 2019.
- [37] Y. Bengio, J. Louradour, R. Collobert, and J. Weston, "Curriculum learning," in *Proceedings of the 26th Annual International Conference on Machine Learning*, p. 4148, Association for Computing Machinery, 2009.
- [38] S. Racaniere, A. K. Lampinen, A. Santoro, D. P. Reichert, V. Firoiu, and T. P. Lillicrap, "Automated curricula through setter-solver interactions," 2019.
- [39] B. Yamauchi, "A frontier-based approach for autonomous exploration," in *Proceedings 1997 IEEE International* Symposium on Computational Intelligence in Robotics and Automation CIRA'97. 'Towards New Computational Principles for Robotics and Automation', pp. 146–151, July 1997.
- [40] B. Yamauchi, "Frontier-based exploration using multiple robots," in *Proceedings of the Second International Con*ference on Autonomous Agents, p. 4753, Association for Computing Machinery, 1998.
- [41] D. Holz, N. Basilico, F. Amigoni, and S. Behnke, "Evaluating the efficiency of frontier-based exploration strategies," in *ISR 2010 (41st International Symposium on Robotics) and ROBOTIK 2010 (6th German Conference on Robotics)*, pp. 1–8, June 2010.
- [42] I. Higgins, L. Matthey, A. Pal, C. Burgess, X. Glorot, M. Botvinick, S. Mohamed, and A. Lerchner, "betavae: Learning basic visual concepts with a constrained variational framework.," *ICLR*, vol. 2, no. 5, p. 6, 2017.
- [43] G. Koch, R. Zemel, and R. Salakhutdinov, "Siamese neural networks for one-shot image recognition," in *ICML deep learning workshop*, vol. 2, 2015.

- [44] H. Bharadhwaj, S. Yamaguchi, and S.-i. Maeda, "Manga: Method agnostic neural-policy generalization and adaptation," *arXiv preprint arXiv:1911.08444*, 2019.
- [45] Y. Bengio, J. Louradour, R. Collobert, and J. Weston, "Curriculum learning," in *Proceedings of the 26th annual international conference on machine learning*, pp. 41–48, ACM, 2009.
- [46] A. Paszke, S. Gross, S. Chintala, G. Chanan, E. Yang, Z. DeVito, Z. Lin, A. Desmaison, L. Antiga, and A. Lerer, "Automatic differentiation in pytorch," 2017.
- [47] A. Paszke, S. Gross, F. Massa, A. Lerer, J. Bradbury, G. Chanan, T. Killeen, Z. Lin, N. Gimelshein, L. Antiga, et al., "Pytorch: An imperative style, high-performance deep learning library," in Advances in Neural Information Processing Systems, pp. 8024–8035, 2019.
- [48] D. P. Kingma and J. Ba, "Adam: A method for stochastic optimization," *arXiv preprint arXiv:1412.6980*, 2014.

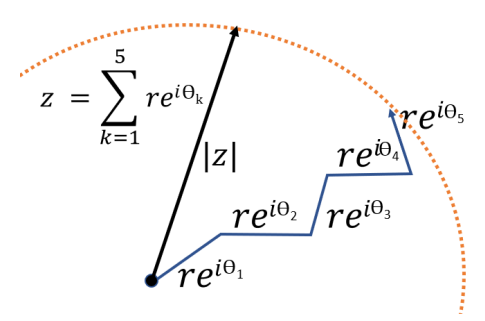


Fig. 7: The setting for the proof of Lemma V.1. The blue jagged line denotes a random walk in 2D free space where the agent takes a step of size r (We take r=1 for convenience and without any loss of generality of the result) at every timestep in any direction  $\theta$ . So,  $re^{i\theta_k}$  is the random variable in the complex plane corresponding to the  $k^{th}$  step.

#### **APPENDIX**

## VIII. PROOFS OF LEMMAS

#### A. Lemma V.1

*Proof.* In a plane, consider the sum of t 2D vectors with random orientations. For convenience, we use the phasor notation, and so assume the phase of each vector to be random. Starting at some point (let's call it the origin  $z_0$ ), we assume t steps are taken in an arbitrary direction, which is equivalent to assuming that the angle  $\theta$  of the phasors is uniformly distributed in  $[0, 2\pi)$ . The position  $z_t$  in the complex plane after t steps is:

$$z_t = \sum_{k=1}^t e^{i\theta_k}$$

The square of the absolute value of  $z_t$  is:

$$|z_t|^2 = \sum_{k=1}^t e^{i\theta_k} \sum_{m=1}^t e^{-i\theta_m} = t + \sum_{k=1, m=1, k \neq m} \sum_{k=1}^t e^{i(\theta_k - \theta_m)}$$

Now, we calculate the expected value of the  $|z_t|^2$  variable by noting that since  $\theta_k$  and  $\theta_m$  are randomly sampled in  $[0, 2\pi)$ with uniform probability, the displacements  $e^{i\theta_k}$  and  $e^{i\theta_m}$  are random variables, so their difference corresponding to  $\theta_k - \theta_m$ is also a random variable and has an expected value (mean)

$$\mathbb{E}_{\theta}|z_t|^2 = \mathbb{E}_{\theta_k,\theta_m \sim [0,2\pi)} \left( t + \sum_{k=1,m=1,k\neq m} \sum_{t=1}^t e^{i(\theta_k - \theta_m)} \right)$$

$$\mathbb{E}_{\theta}|z_t|^2 = t \implies |z_t|_{rms} = \sqrt{t}$$

So, the average (root-mean-square) distance traversed after t steps starting at some  $z_0$  in the 2D plane is  $\sqrt{t}$ **OED** 

## B. Lemma V.5

*Proof.* Given  $R_3 = k^* + \sqrt{T - k^*}$  and  $R_1 = \sqrt{T}$ . Let us first consider the difference  $R_3^2 - R_1^2$  below:

$$R_3^2 - R_1^2 = (k^* + \sqrt{T - k^*})^2 - (\sqrt{T})^2$$

$$= (k^*)^2 + T - k^* = 2k^*\sqrt{T - k^*} - T$$

$$= k^*(k^* - 1 + 2k^*\sqrt{T - k^*})$$

$$> 0 \quad \forall k^* \in (1, T)$$

Hence,

$$R_3^2 - R_1^2 > 0 \quad \forall k * \in (1, T)$$
$$\implies R_3 > R_1 \quad \forall k * \in (1, T)$$

Now, let us consider  $R_2 = \frac{1}{k^*} \sum_{k=0}^{k^*} (k + \sqrt{T - k})$ . For computing this, we can consider the change of variable  $k \implies$ r such that  $T - k = r^2$ . So,  $k = T - r^2$ . Hence we have the following relation:

$$R_2 = \frac{1}{k^*} \sum_{r=\sqrt{T-k^*}}^{\sqrt{T}} (T - r^2 + r)$$

We have,

$$\sum_{r=\sqrt{T-k^*}}^{\sqrt{T}} (T-r^2+r) = T(\sqrt{T}-\sqrt{T-k^*}) - \sum_{r=\sqrt{T-k^*}}^{\sqrt{T}} (r^2-r)$$

Now, 
$$\sum_{r=\sqrt{T-k^*}}^{\sqrt{T}} r^2 = \sum_{r=0}^{\sqrt{T}} r^2 - \sum_{r=0}^{\sqrt{T-k^*}} r^2$$

$$= \frac{1}{6} [\sqrt{T}(\sqrt{T}+1)(2\sqrt{T}+1)$$

$$-\sqrt{T-k^*}(\sqrt{T-k^*}+1)(2\sqrt{T-k^*}+1)]$$

$$= \frac{1}{6} [2T\sqrt{T}+3T+\sqrt{T}$$

$$-2(T-k^*)\sqrt{T-k^*}-3(T-k^*)-\sqrt{T-k^*}]$$

$$= \frac{1}{6} [2T\sqrt{T}+\sqrt{T}$$

$$-2(T-k^*)\sqrt{T-k^*}+3k^*-\sqrt{T-k^*}]$$

$$\sum_{r=\sqrt{T-k^*}}^{\sqrt{T}} r = \frac{1}{2} [\sqrt{T}(\sqrt{T}+1) - \sqrt{T-k^*}(\sqrt{T-k^*}+1)]$$

$$= \frac{1}{2} [T + \sqrt{T} - (T-k) - \sqrt{T-k^*}]$$

$$= \frac{1}{2} [\sqrt{T} + k^* - \sqrt{T-k^*}]$$

So, finally,

$$6 \sum_{r=\sqrt{T-k^*}}^{\sqrt{T}} (r^2 - r) = 2T\sqrt{T} + \sqrt{T} - 2(T - k^*)\sqrt{T - k^*}$$

$$+ 3k^* - \sqrt{T - k^*} - \sqrt{T} - k^* + \sqrt{T - k^*}$$

$$= 2T\sqrt{T} - 2(T - k^*)\sqrt{T - k^*} + 2k^*$$

Hence, 
$$R_2$$
 is given by 
$$R_2=\frac{1}{6k^*}[4T\sqrt{T}-4T\sqrt{T-k^*}-k^*\sqrt{T-k^*}-2k^*]$$
 Considering  $R_3-R_2$ , we have, 
$$6k^*(R_3-R_2)=6(k^*)^2+(7k^*+4T)\sqrt{T-k^*}-4T\sqrt{T}+2k^*$$

Let,  $f(k^*) = 6k^*(R_3 - R_2) = 6(k^*)^2 + (7k^* + 4T)\sqrt{T - k^*} - (7k^* + 4T)\sqrt{T - k^*}$  $4T\sqrt{T} + 2k^*$ . By treating  $k^*$  as continuous, we find that the gradient  $\frac{\partial f}{\partial k^*} > 0 \ \forall k^* \in (0,T]$ . Also, the value  $f(k^* = 0) =$ 0. Hence, we have proved that  $R_3 > R_2 \ \forall k \in [1, T]$ . QED

# Algorithm 2 The complete proposed Algorithm

```
1: procedure OVERALL(GCP \pi_{\theta}, Prior p(z), S, f_{\psi}(\cdot),
     IsReachable(\cdot), H_0, N, \epsilon, \delta)
 2:
         p_{\phi} = p(z)
         Initialize ReachNet(\cdot,\cdot;k) where k = \{K,...,1\}
 3:
 4:
         Def K = H_0 * N lists for p_k.
         Def Global ReachDataset = \{\} //to train ReachNet
 5:
         for episodes = 1 to N do
 6:
              Sample initial state s_0 \sim S_0, encode z_0 = f_{\psi}(s_0)
 7:
              Sample latent goal z_g from p_{\phi} = p_{skewed}
 8:
              \hat{z}^* = z_0
 9:
             //Apply our idea after some training
10:
              if episodes \geq N/4 then
11:
                  for k = K - 1, ..., 1 do
12:
                       Set the value of IsReachable(z_0; k)
13:
                  k^* = \arg\max_{k} (IsReachable(z_0; k))
14:
                  Choose z_{k^*} = \arg\min_{z \sim p_{k^*}} ||z - z_g||_2
Exec \pi_{\theta}(z_0; z_{k^*}), reach \hat{z}^* s.t. ||\hat{z}^* - z_{k^*}|| \approx 0
15:
16:
              Set H = H_0 * episodes // Curriculum
17:
              for t = 0, ..., H - 1 do
18:
                  if t == 0 then
19:
20:
                       Select a_t \sim \pi_{\theta}(\hat{z}^*; z_q) and execute it
                  if t > 0 then
21:
                       Select a_t \sim \pi_{\theta}(f_{\psi}(s_t); z_q) and execute it
22:
                  The env transitions to state s_{t+1} \sim p(\cdot|s_t, a_t)
23:
                  Store (s_t, a_t, s_{t+1}, z_g, t+1) in replay buffer \mathcal{R}
24:
                  Sample transition (s, a, s', z_a^h, k) \sim \mathcal{R}
25:
                  Encode z = f_{\psi}(s), z' = f_{\psi}(s')
26:
                  Compute the latent reward r = -||z' - z_a^h||
27:
                  Minimize B.E. with (z, a, z', z_q^h, k, r)
28:
              //Append to the dataset for training the ReachNet
29:
              for t_1 = 0, ..., H - 1 do
30:
                  for t_2 = 0, ..., H - 1 do
31:
                       if t_1 \neq t_2 then
32:
                           ReachDataset.add((z_{t_1}, z_{t_2}, |t_1 - t_2|))
33:
             // Samples states to add in replay buffer \mathcal{B}
34:
              for t = 0, ..., H - 1 do
35:
                  for i = 0, ..., k - 1 do
36:
                       Sample future states s_{h_i}, t \le h_i - 1 \le H - 2
37:
                       Store (s_t, a_t, s_{t+1}, f_{\psi}(s_{h_i}), h_i + 1) in \mathcal{B}
38:
              Construct skewed dist. p_{skewed} from \mathcal{B} (Skew-Fit)
39:
              Train the encoder using p_{skewed}
40:
              Train ReachNet(\cdot,\cdot;k) using ReachDataset
41:
```

## IX. THE COMPLETE ALGORITHM AND SUBROUTINES

## X. DETAILS ABOUT THE ENVIRONMENTS

• Pointmass Navigation (Image-based): This is a 2D environment where an object (circular with diameter 1cm) must learn to navigate a square-shaped arena from an initial location to a goal location in the presence of obstacles. The obstacle is a U-shaped wall in the center. The agent must plan a temporally extended path that

Algorithm 3 Subroutines of the overall algorithm (forward referenced in Alg. 1)

```
1: procedure StoreandTrain(())
        The env transitions to state s_{t+1} \sim p(\cdot|s_t, a_t)
2:
3:
        Store (s_t, a_t, s_{t+1}, z_q, t+1) in replay buffer \mathcal{R}
        Sample transition (s, a, s', z_a^h, k) \sim \mathcal{R}
4:
        Encode z = f_{\psi}(s), z' = f_{\psi}(s')
5:
        Compute the latent reward r=-||z'-z_g^h|| Minimize Bellman Error with (z,a,z',z_g^h,k,r)
6:
7:
    procedure APPENDTODATASET(ReachDataset \mathcal{D})
8:
9:
        for t_1 = 0, ..., H-1 do
10:
             for t_2 = 0, ..., H - 1 do
                  if t_1 \neq t_2 then
11:
                       ReachDataset.add((z_{t_1}, z_{t_2}, |t_1 - t_2|))
12:
    procedure SampleFutureStates(\mathcal{B})
13:
        for t = 0, ..., H - 1 do
14:
             for i = 0, ..., k - 1 do
15:
                  Sample future states s_{h_i}, t \leq h_i - 1 \leq H - 2
16:
17:
                  Store (s_t, a_t, s_{t+1}, f_{\psi}(s_{h_i}), h_i + 1) in \mathcal{R}
```

would occassionally involve moving away from the goal. This is a 2D environment with a continuous action space, and the agent has access to images from a top-down view. The observations and goals for evaluation are specified as 48x48 RGB images. The total dimensions of the arena are 8cmx8cm, and the thickness of the U-shaped wall is 1cm. The action space is a 2D vector  $(v_x, v_y)$  consisting of velocity components in the x and y dimensions. For evaluation, the final (x,y) position of the center of the object at the end of the episode is computed from the actual (x,y) position of the goal. During training, the only reward is the distance (L2 norm) between the current latent state z' and the latent goal state $z_g^h$ ,  $r = -||z' - z_g^h||$  as shown in the Algorithm.

Fetch Slide (State-based): A Fetch robot arm must be controlled to push and slide a puck on the table such that it reaches a certain goal location. It is ensured that sliding must happen (and not just pushing) because the goal location is beyond the reach of the arm's end-effector. We make this environment significantly difficult by reducing the default friction coefficient by a factor of 2, to have  $\mu = 0.3$ . The workspace has a dimension of 10cmx30cm. Since, we assume access to the state of the simulator here, goals are specified as the desired (x, y) position of the puck. The observations are specified as a vector containing the absolute position of the gripper, and the relative position of the object and target goal position. Actions are 3D vectors specifying the desired relative gripper position at the next timestep. Rewards during training are sparse and they do access the ground-truth simulator states (unlike the image based environments where we use latent rewards):  $r(s, a, g) = -\mathbb{I}\{|g - s'| \le \epsilon\}$ , where I is the indicator function, g denotes the goal state, s'denotes the next state after executing action a in state s.

- Gridworld Locked Door Navigation (*Image-based*): A point agent must navigate a maze to pick up a key, open a locked door, and navigate to a goal location on the other side of the door. This is a 2D environment, and the agent has access to images from a top-down view. At each time-step, the agent has the option to choose from six actions (so, discrete action space). The dimensions of the overall grid are 8x8. The agent receives a +1 reward only after completing the entire task, and the reward is 0 at all other timesteps.
- Sawyer Pick (Image-based): A MuJoCo powered 7-DoF Sawyer robot arm must be controlled to pick a puck from a certain location and lift it to a target location above the table. The observations and goals for evaluation are specified as 84x84 RGB images. The workspace dimensions of the table are  $10 \text{cm} \times 15 \text{cm}$  (x and y dimensions). However, the robot is constrained to move only in the y and z dimensions. The dimension that can be accessed in the yz plane is 15cmx15cm. The object to be picked up is a cube of edge length 1.5cm. The robot is position controlled and, action space is continuous and is a vector  $(a_x, a_z, a_{qrip})$  denoting relative position of the end-effector at the next timestep in yz plane, and the separation between the gripper fingers. For evaluation, the final (y, z) position of the center of the object at the end of the episode is computed from the actual (y, z) position of the object in the goal image. During training, the only reward is the distance (L2 norm) between the current latent state z' and the latent goal state  $z_g^h, r = -||z' - z_g^h||_2$  as shown in the Algorithm.
- Sawyer Push (Image-based): A MuJoCo powered 7-DoF Sawyer robot must push a puck to a certain location with the help of its end-effector. The observations and goals for evaluation are specified as 84x84 RGB images. The workspace dimensions of the table are 20cmx30cm. The puck has a radius of 6cm. The robot is position controlled, the action space is continuous and is a vector  $(a_x, a_y)$  denoting relative position of the end-effector at the next timestep in xy plane. For evaluation, the final (x, y) position of the center of the object at the end of the episode is computed from the actual (x, y) position of the puck in the goal image. During training, the only reward is the distance (L2 norm) between the current latent state z' and the latent goal state  $z_g^h$ ,  $r = -||z' z_g^h||$  as shown in the Algorithm.
- Sawyer Push and Reach (Image-based): A MuJoCo powered 7-DoF Sawyer robot arm must be controlled to push a puck to a target location, and move its end-effector to a (different) target location. The observations and goals for evaluation are specified as 84x84 RGB images. The workspace dimensions of the table are 25cmx40cm. The puck has a radius of 6cm. The robot is position controlled, the action space is continuous and is a vector  $(a_x, a_y)$  denoting relative position of the end-effector at the next timestep in xy plane. For evaluation, the concatenation of the final (x,y) position of the center of the puck, and

- the (x,y) position of the end-effector at the end of the episode is computed from the actual (x,y) position of the center of the puck, and the (x,y) position of the end-effector in the goal image. During training, the only reward is the distance (L2 norm) between the current latent state z' and the latent goal state  $z_g^h$ ,  $r=-||z'-z_g^h||$  as shown in the Algorithm.
- Franka Panda Peg in a Hole (Image-based; Real robot); A real Franka Panda arm must be controlled to place a peg in a hole. The agent is velocity controlled and has access to state information of the robot. The states observed at each time-step are 6-tuples containing the positions and velocities of the end-effector  $(x, y, z, v_x, v_y, v_z)$ . The reward function is defined to be the negative of the distance from the center of bottom of the peg to the center of the bottom of the hole. There is an additional heavy reward penalty for 'collision' and a mild penalty for 'contact.' The home position of the panda arm (to which it is initialized) is such that the distance from the center of the bottom of the peg to the center of the bottom of the hole is 0.35 meters. The heavy penalty for collision is -10 and the mild penalty for contact is -1.